Heart and Vessels (2019) 34:427–434
https://doi.org/10.1007/s00380-018-1271-9

ORIGINAL ARTICLE

Morphological characteristics of optical coherence tomography defined plaque fissure in patients with acute coronary syndrome

Mayank Goyal[1] · Sang Wook Kim[1] · Sundeep Mishra[2] · Saima Sharmin[1] · Hoyoun Won[1] · Iksung Cho[1] · Moon Ki Jung[1] · Seung Yong Shin[1] · Kwang Je Lee[1] · Tae Ho Kim[1] · Chee Jeong Kim[1] · Wang Soo Lee[1]

Received: 28 January 2018 / Accepted: 28 September 2018 / Published online: 4 October 2018

Abstract

We assessed the plaque disruption in 245 consecutive patients with acute coronary syndrome undergoing percutaneous coronary intervention. The plaque fissure was diagnosed with optical coherence tomography, and intravascular ultrasound was used to determine arterial remodeling. Of them, 26 fissures were found in this study. The definite fissure was seen in 17 (65.4%) and probable fissure was seen in 9 (34.6%) patients. In 18 (69.2%), plaque fissure component was lipidic or thin-capped fibroatheroma. Eighteen (69.2%) of fissured plaque were seen within 30 mm of coronary ostium. Combined plaque fissure with plaque rupture/erosion was seen in 21 (80.8%) cases. The isolated fissure was seen in 5 (19.2%). Compared to the maximal necrotic core site of the ruptured plaque, the fissure site showed a smaller %necrotic core ($p=0.012$), however, greater in fissure site than minimal lumen area site ($24.93 \pm 11.50\%$ vs $15.34 \pm 10.40\%$, $p<0.0001$). The remodeling index was higher at fissure site as compared to minimal lumen area site (1.02 ± 0.22 vs 0.94 ± 0.27; $p=0.047$), but similar to the rupture plaque ($p=0.31$). The frequency of positive remodeling was 34.6% (9/26) at the plaque fissure. Although the plaque fissure can be interchangeable with the rupture in acute coronary syndrome, the limited extension to the small lipid core might and less positive remodeling provoke a fissuring of the plaque. Further study is necessary to assess the plaque fissure.

Keywords Plaque fissure · Optical coherence tomography · Acute coronary syndrome

Abbreviations

ACS	Acute coronary syndrome
EEM	External elastic membrane
ECG	Electrocardiogram
IVUS	Intravascular ultrasound
MLA	Minimal lumen area
NSTEMI	Non-ST elevation myocardial infarction
OCT	Optical coherent tomography
PCI	Percutaneous coronary intervention
P&M	Plaque and media
QCA	Quantitative coronary angiography
TIMI	Thrombolysis in Myocardial Infarction
STEMI	ST elevation myocardial infarction
PR	Plaque rupture
PE	Plaque erosion
TCFA	Thin-capped fibroatheroma
VH-IVUS	Virtual-Histology Intravascular Ultrasound

Introduction

A plaque fissure has been assumed to be the cause of acute coronary syndrome (ACS). From erosions of the luminal surface to deep plaque rupture extending into the lipid core plays a fundamental role in development of ACS [1–3]. The plaque fissure is seen in 10–15% of sudden coronary death cases [4]. Pathologically 'fissure' is defined as a lateral tear in an eccentric plaque with the underlying small necrotic core. And scanning electron microscopy revealed the areas of plaque fissuring [5]. However, the term of a plaque fissure was used mutually with the plaque rupture [6]. Only one

Sang Wook Kim and Wang Soo Lee equally contributed to this article as correspondence.

✉ Sang Wook Kim
swkimcv@cau.ac.kr

✉ Wang Soo Lee
wslee1227@cau.ac.kr

[1] Heart Research Institute, Cardiovascular-Arrhythmia Center, College of Medicine, Chung-Ang University Hospital, 102, Heukseok-ro, Dongjak-gu, Seoul 06973, Korea

[2] All India Institute of Medical Science, New Delhi, India

case report was available describing a plaque fissure formation after balloon angioplasty [7].

Recent studies have shown that Optical coherence tomography (OCT) is useful in assessing vulnerable plaque features in vivo due to high resolution [8, 9]. OCT allows us to demonstrate culprit lesion morphologies in detail including types of plaque, fibrous cap thickness, and the frequency of thin-capped fibroatheroma (TCFA) and thrombus in ACS [10]. However, a few clinical study was reported about the fissure of the atherosclerotic coronary plaque.

The objectives of this study were to assess the plaque fissure which can be differentiated from the plaque rupture in patients with acute coronary syndrome.

Methods

Overall 245 consecutive patients admitted to the hospital due to acute coronary syndrome and underwent percutaneous coronary intervention (PCI) with intravascular ultrasound (IVUS) and OCT were enrolled. Patients with congestive heart failure, renal insufficiency (baseline serum creatinine > 1.8 mg/dL (133 μmol/L)), debulking or plaque modification procedures before intravascular imaging, and extremely tortuous vessels or heavy calcification which caused the difficulty in advancing the imaging catheters were excluded (Fig. 1).

ST elevation myocardial infarction (STEMI) was diagnosed based on continuous chest pain for at least 30 min, arrival at the hospital within 6 h from the onset of symptoms, ST-segment elevation > 0.1 mV in two or more contiguous leads or new left bundle-branch block on the 12-lead electrocardiogram (ECG), and elevated cardiac markers (plasma creatine kinase-myocardial band or troponin I). Non–ST-segment elevation myocardial infarction (NSTEMI) was defined as ischemic symptoms in the absence of ST-segment elevation on the ECG with elevated cardiac markers. Unstable angina pectoris (UAP) was defined as new onset/accelerating chest symptoms on exertion or rest angina within 2 weeks. Thrombus aspiration was performed prior to IVUS and OCT imaging using an aspiration catheter (Thrombuster®, Kaneka Co, Japan) according to operator discretion, but typically for large thrombi in the setting of an ST-segment elevation myocardial infarction (STEMI). Hypertension was defined as systolic blood pressure ≥ 140 mmHg or diastolic blood pressure ≥ 90 mmHg or current use of antihypertensive treatment. Diabetes mellitus was defined as hemoglobin A1C ≥ 6.5mg/dL or medication treatment for diabetes mellitus. Dyslipidemia was defined as having total cholesterol ≥ 240 mg/dl, low-density lipoprotein cholesterol ≥ 160 mg/dl, HDL cholesterol < 40 mg/dl, or self-reported use of lipid-lowering drugs. The protocol was approved by the institutional review board, and written consent was obtained from all patients.

Coronary angiography was performed after 200 μg of intracoronary nitroglycerin. All angiograms were independently analyzed with an automated edge-detection algorithm (AI 2000; GE Medical) using standard protocols. Lesion measurements were performed in the "worst" view, with the end-diastolic frame selected for analysis. Minimal luminal diameter, % diameter stenosis and reference vessel diameter were measured before the coronary intervention. A coronary stenosis was considered clinically significant if > 50% in diameter.

A commercially available frequency domain OCT system (C7-XR or Ilumien System, Light Lab Imaging, Inc., St. Jude Medical, Westford, Massachusetts) and a 0.014-in. wire-type imaging catheter (ImageWire, St. Jude

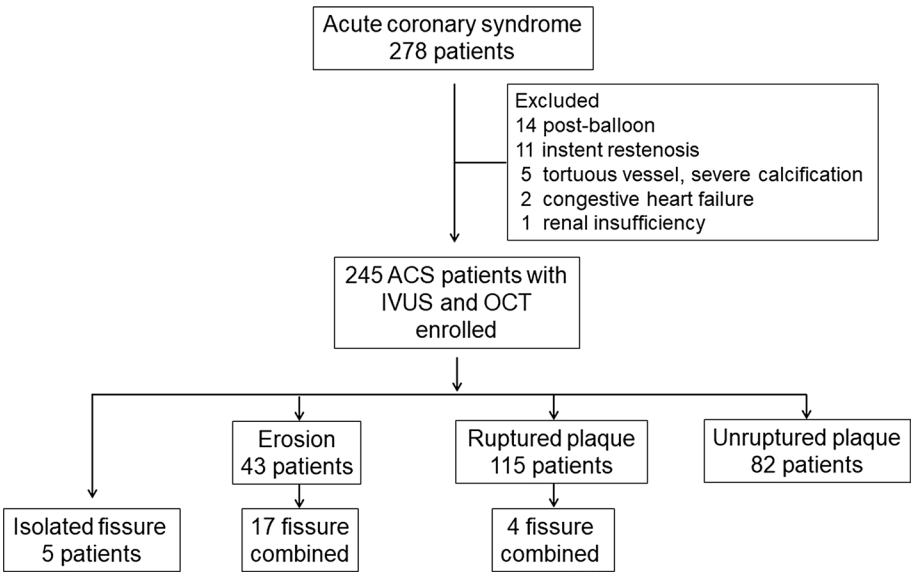

Fig. 1 Flow chart of the study

Medical, Westford, Massachusetts) were used. Motorized ImageWire pull-back at 10mm/sec was performed during simultaneous injection of a viscous iso-osmolar contrast solution. The definite fissure was defined as a linear tear in the luminal surface of plaque (Figs. 2, and 3a). The probable fissure was defined as the lateral tear of the luminal surface in one frame of OCT (Fig. 3b). However, an OCT image motion artifact such as a tangential and seam-line artifacts and vessel structure which create a mimicking linear structure were excluded. The definite and probable plaque erosion was defined as reported previously[11, 12]. OCT-identified TCFA was defined as a fibrous cap thickness ≤ 65 μm at the thinnest part and an angle of the lipid $\geq 180°$. The culprit lesion was identified on the basis of the ECG, stress test, echocardiography, and angiographic findings which showed a lesion with complex features including a thrombus, ulcer with overhanging edges, extraluminal contrast, dissection or intraluminal flap, multiple irregularities or acute occlusion. OCT plaque composition was analyzed as defined previously [13]. IVUS imaging was performed in all the patients after OCT examination. All OCT images were analyzed using a certified Offline Review Workstation (St. Jude Medical, Westford, Massachusetts) by two experienced analysts (YMJ and DWK) who were blinded to patient information.

A commercially available VH-IVUS system (Volcano Therapeutics, Rancho Cordova, California, USA) and 20 MHz transducers were used for all IVUS examinations. Greyscale IVUS analysis was performed according to criteria of the American College of Cardiology clinical expert consensus document on IVUS using planimetry software (Echoplaque 4, INDEC Systems Inc., Mountain View, CA) [14].

IVUS imaging was performed after intracoronary administration of 200 μg of nitroglycerin. The IVUS catheter was advanced 10 mm distal to the target lesion, and imaging was performed retrograde back to the aorto-ostial junction using an ECG-gated automatic pullback device. Studies were recorded onto electronic media for off-line analysis. VH-IVUS plaque composition and lesion phenotype were assessed after defining the two standard VH-IVUS regions-of-interest—inner border (lumen, excluding IVUS-detectable thrombus) and outer border (external elastic membrane). Pathologic intimal thickening (PIT), TCFA, and fibrotic or fibrocalcific plaque were defined as published [15]. VH-TCFA was a fibroatheroma without evidence of a fibrous cap and $> 10\%$ confluent necrotic core (NC) with $> 30°$ NC abutting the lumen in ≥ 3 consecutive frames. Positive remodeling was defined as a remodeling index (lesion/reference EEM [external elastic membrane] area) ≥ 1.05,

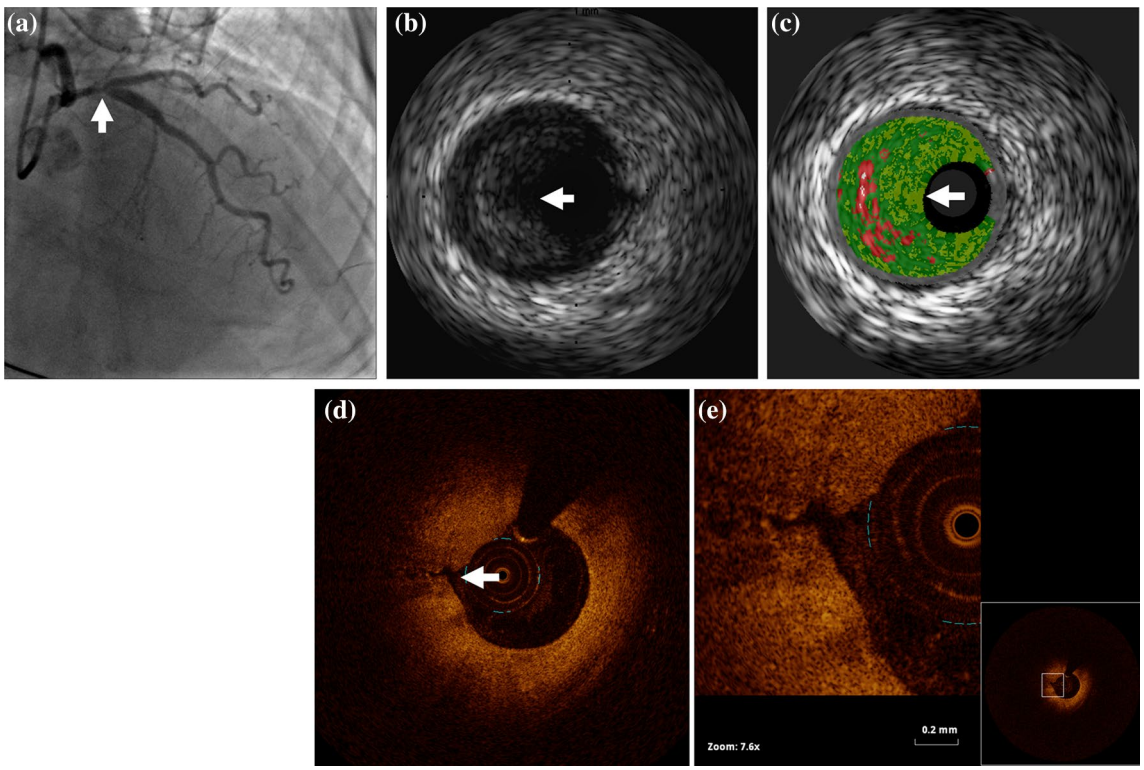

Fig. 2 OCT and IVUS image of definite fissure. **a** Angiogram showing tight stenosis in the proximal portion of left anterior descending artery (white arrow). **b**, **c** IVUS image showing the fibrotic plaque (white arrow). **d**, **e** OCT image showing the plaque fissure (white arrow)

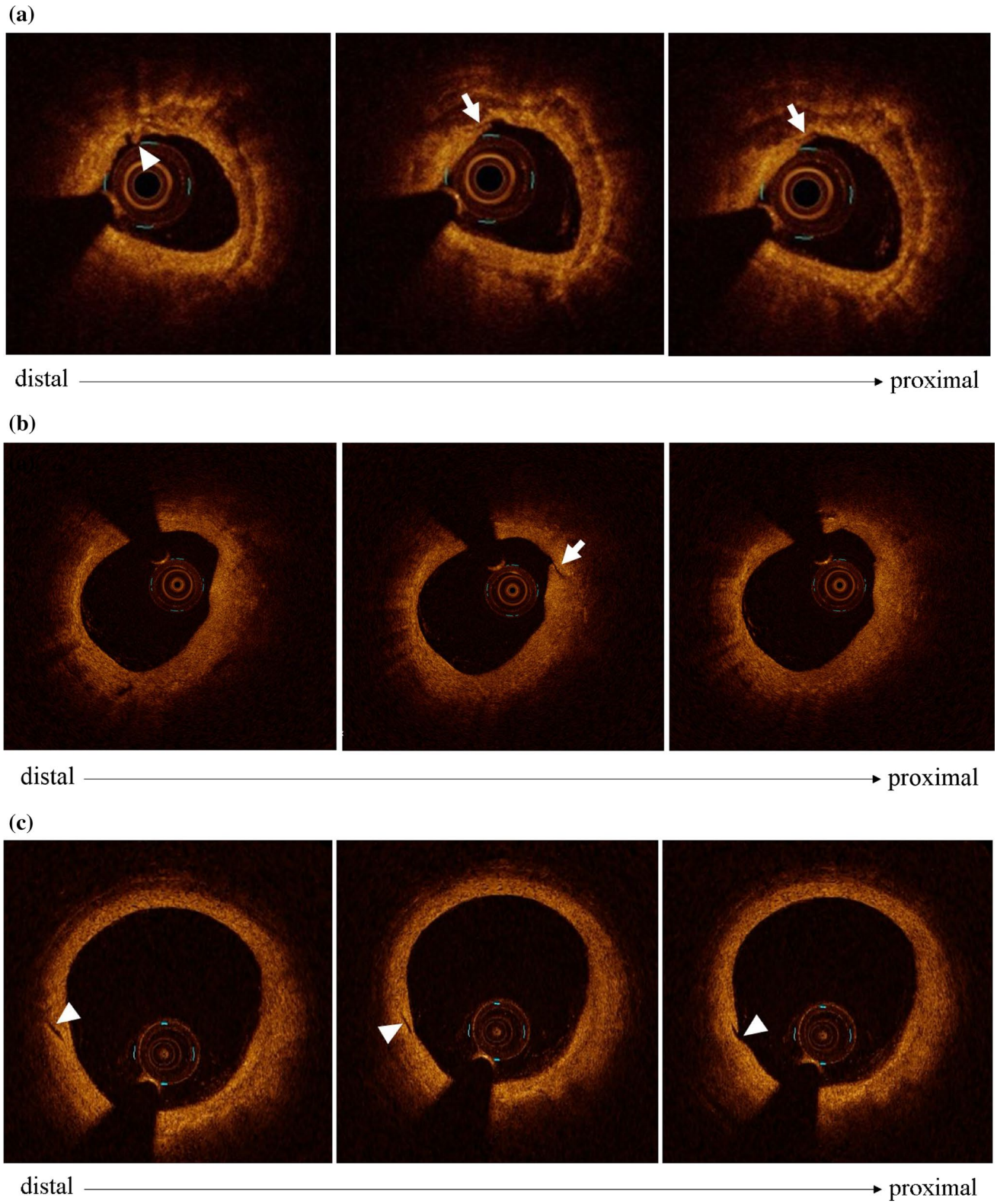

Fig. 3 Comparative OCT findings of the coronary fissure and vasa vasorum. **a** Definite fissure with intimal tear (white arrow) was found at the base of plaque erosion with white thrombus (arrow head). **b** Probable fissure with intimal tear (white arrow) in one frame of OCT. **c** Comparative findings of vasa vasorum (arrow head)

intermediate remodeling was between 0.95 and 1.05, and a remodeling index ≤0.95 was negative remodeling. Culprit lesions on VH-IVUS and OCT studies were compared using reproducible axial landmarks (usually the aorto-ostial junction, a large proximal side branch, and/or reference segment calcific deposits) and known pullback speeds.

Results are expressed as mean ± SD or number (%). In comparing two independent samples, Student *t* test (parametric statistical test) and Wilcoxon rank-sum test (nonparametric statistical test) are used to compare continuous variable. When comparing two matched samples, paired Student's *t* test (parametric statistical test) was performed to compare continuous variables. Intraobserver and interobserver variability was estimated by the Cohen's kappa and Cronbach's alpha. All analysis were performed using standard statistical software (SPSS version 18.0; IBM, Chicago, Illinois, USA), and $p < 0.05$ was considered statistically significant.

Results

Baseline characteristics of the study population are shown in Table 1. 26 patients (26 lesions) were found to have the plaque fissure. It showed male preference (76.9%) and hypertension was combined in 50%. And the left anterior descending artery was frequently associated with the plaque fissure. Compared to the non-fissure, the fissure group showed the higher incidence of NSTEMI, and less unstable angina and STEMI.

OCT finding at the site of plaque fissures is shown in Table 2. The definite fissure was seen in 17/26(65.4%) and probable fissure was seen in 9/26(34.6%). The average length of the fissure was 216 ± 158 μm, average width of the fissure was 44 ± 20 μm. The plaque component of fissure site was lipidic in 16/26 (61.5%), TCFA in 2/26 (7.7%), 4/26 (15.4%) each having fibrous or calcific. Combined fissure with plaque rupture/erosion was seen in 21/26 (80.8%) cases. Associated plaque rupture/erosion was located proximally in 10/21 (47.6%), distal in 8/21 (38.1%), and 3/21 (14.3%) occur at the same site of the plaque fissure. Isolated plaque fissure (not combined with PR/PE) was seen in remaining 5/26 (19.2%) cases.

Intracoronary thrombus was found in 16/26 (61.5%); red thrombus was most frequent in 8/26 (30.8%), white thrombus in 5/26 (19.2%), both red and white thrombus in 3/26 (11.5%) and no detectable thrombus in 10/26 (38.5%). The calcified nodule was seen in 2 patients, however, it was not associated with culprit lesion or the coronary fissure.

Table 3 showed the result of the greyscale and virtual histology intravascular ultrasound. 26 plaque fissures were compared with 115 ruptured plaque which were identified by the OCT and VH-IVUS. On greyscale and VH-IVUS, the external elastic membrane area of reference site was similar in both of plaque fissure and maximal necrotic core site of ruptured plaque. And the lumen area and plaque burden were similar ($p = 0.37$, $p = 0.21$, respectively). At the fissure site, %necrotic core (NC) was smaller than ruptured plaque (24.93 ± 11.50% vs 31.63 ± 10.50%, $p = 0.012$), however, greater in fissure site than in MLA site (24.93 ± 11.50% vs 15.34 ± 10.40%, $p < 0.0001$). 69.2%(18/26) of the plaque fissure were distributed within 30mm of the coronary ostium (Fig. 4). The remodeling index was higher at the fissure site as compared to the MLA site ($p = 0.047$), but similar with ruptured plaque ($p = 0.31$). The frequency of positive remodeling was 9/26 (34.6%) at the fissure site.

Interobserver agreements for the detection of plaque fissure was $\kappa = 0.89$. The intraobserver and interobserver agreements of the fissure length were $\alpha = 0.99$ and $\alpha = 0.99$, respectively, and the agreements for the width were $\alpha = 0.96$ and $\alpha = 0.98$, respectively.

Table 1 Baseline characteristics

	Fissure ($n = 26$)	Ruptured plaque ($n = 115$)	*p* value
Age (years)	60 ± 12.3	61 ± 10.7	0.78
Male gender, *n* (%)	20 (76.9)	91 (79.1)	0.85
Diabetes mellitus, *n* (%)	3 (11.5)	25 (21.7)	0.16
Hypertension, *n* (%)	13 (50)	52 (45.2)	0.41
Current smoker, *n* (%)	8 (30.8)	40 (34.7)	0.97
Dyslipidemia, *n* (%)	3 (11.5)	22 (19.1)	0.55
Clinical presentation, *n* (%)			0.03
Unstable angina	11 (42.3)	65 (56.5)	
Non-ST elevation MI	8 (30.8)	11 (9.6)	
ST elevation MI	7 (26.9)	39 (33.9)	
Target vessel, *n* (%)			0.22
LAD	17 (65.4)	68 (59.1)	
RCA	7 (26.9)	29 (25.2)	
LCX-OM	2 (7.6)	18 (15.7)	
Quantitative coronary angiography			
Lesion length (mm)	21.46 ± 6.6	20.7 ± 6.9	0.6
Minimal lumen diameter (mm)	1.91 ± 0.99	2.15 ± 1.38	0.5
Diameter stenosis (%)	74 ± 16.18	78 ± 16.9	0.74
Reference diameter (mm)	3.12 ± 0.71	3.24 ± 0.58	0.9
TIMI flow, *n* (%)			0.08
0	4 (15.4)	31 (27.0)	
1	0 (0)	3 (2.6)	
2	5 (19.2)	35 (30.4)	
3	17 (65.4)	46 (40.0)	

Values are presented as mean ± SD or percentages

MI myocardial infarction, *LAD* left anterior descending artery, *LCX-OM* left circumflex artery-obtuse marginal, *RCA* right coronary artery, *TIMI* thrombolysis in myocardial infarction

Table 2 Optical coherence tomographic findings of the plaque fissure

Fissured plaque	
Definite, *n* (%)	17 (65.4)
Probable, *n* (%)	9 (34.6)
Combined with PR or PE	
Combined, *n* (%)	21 (80.8)
Isolated, *n* (%)	5 (19.2)
Average lumen area at fissure site (mm^2)	5.41 ± 3.44
Average fissure length (μm)	216 ± 158
Average fissure width (μm)	44 ± 20
OCT fissure component	
Fibrotic, *n* (%)	4 (15.4)
Lipidic, *n* (%)	16 (61.53)
Calcific, *n* (%)	4 (15.4)
TCFA, *n* (%)	2 (7.7)
Thrombus	
White thrombus, *n* (%)	5 (19.2)
Red thrombus, *n* (%)	8 (30.8)
Both red and white thrombus, *n* (%)	3 (11.5)
No thrombus, *n* (%)	10 (38.5)

Values are presented as mean ± SD or percentages

TCFA thin-capped fibroatheroma, *PR* plaque rupture, *PE* plaque erosion

Discussion

The main finding of this study are as follows; (1) the plaque fissure is often combined with plaque disruption including the plaque rupture and erosion as like a multiple rupture. (2) A plaque fissure can occur at the sites with smaller necrotic core and less positive remodeling. (3) The pathophysiologic mechanism might be similar to the plaque rupture/erosion which is mostly located in the proximal coronary artery.

Histopathological studies have shown that site of coronary thrombosis on the atherosclerotic plaque was influenced by variation in the mechanical strength of thin cap and local flow conditions [16]. The transition to an unstable plaque is characterized by the accumulation of a large necrotic core, containing extracellular lipids, macrophages, and often microcalcifications. Long-term repetitive phasic activation of inflammatory activity may weaken the plaque core and increase its vulnerability to fracture leading to the multilayered thrombi and multiple simultaneous plaque ruptures. However, these multiple healed plaque ruptures are typically responsible for high-grade coronary arterial stenosis [17]. Most of the unstable plaques tend to cluster within proximal portion of major epicardial coronaries due to multiple mechanical and hemodynamic stresses [18–21]. Ruptured plaques frequently occur in the context of OCT-TCFAs and show features of intimal tearing, disruption, or dissection of the cap. When injected with optically transparent crystalloid or radiocontrast media, these defects may have little or no OCT signal and may appear as a cavity [13].

The low resolution of IVUS precludes the evaluation of a plaque fissure. However, the imaging studies have used an OCT to evaluate plaque erosion in the pathophysiology of ACS in vivo [11, 12, 21]. The plaque fissure is defined as a

Table 3 Comparison of IVUS finding at fissure site and ruptured plaque

	Fissure (*n* = 26)	Ruptured plaque (*n* = 115)	*P* value
Proximal reference segment			
EEM area (mm^2)	16.63 ± 5.08	18.27 ± 5.04	0.20
Lumen area (mm^2)	8.94 ± 3.36	9.07 ± 2.81	0.85
Plaque area (mm^2)	7.68 ± 2.78	9.79 ± 6.13	0.12
Lesion site			
EEM area (mm^2)	16.18 ± 5.74	16.60 ± 5.73	0.76
Lumen area (mm^2)	6.16 ± 3.97	5.54 ± 2.65	0.37
Plaque area (mm^2)	10.01 ± 4.08	11.05 ± 4.18	0.29
Plaque burden (%)	62.15 ± 15.52	66.55 ± 9.93	0.21
Fibrotic area (mm^2)	3.72 ± 2.13	4.09 ± 2.50	0.53
Fibrofatty area (mm^2)	0.85 ± 1.15	0.65 ± 0.91	0.38
Necrotic core (mm^2)	1.85 ± 1.36	2.62 ± 1.54	0.04
Dense calcium (mm^2)	0.54 ± 0.58	0.85 ± 0.74	0.08
% Fibrotic area	55.56 ± 18.63	49.28 ± 13.12	0.07
% Fibrofatty area	10.46 ± 9.22	8.54 ± 10.77	0.46
% Necrotic core area	24.93 ± 11.50	31.63 ± 10.50	0.012
% Dense calcium area	7.51 ± 8.01	10.79 ± 7.86	0.09
Remodeling index	1.02 ± 0.22	1.09 ± 0.31	0.31
VH-TCFA, *n* (%)	7 (27)	51 (44.3)	0.09
Minimal lumen area site			
EEM area (mm^2)	13.06 ± 5.67	13.33 ± 4.67	0.81
Lumen area (mm^2)	2.94 ± 1.83	2.67 ± 1.35	0.43
Plaque area (mm^2)	10.14 ± 4.87	10.66 ± 4.25	0.62
Plaque burden (%)	75.86 ± 10.22	79.05 ± 8.57	0.13
Fibrotic area (mm^2)	4.33 ± 2.74	5.09 ± 5.25	0.52
Fibrofatty area (mm^2)	1.57 ± 1.50	1.41 ± 1.30	0.60
Necrotic core (mm^2)	1.31 ± 1.20	1.58 ± 1.10	0.30
Dense calcium (mm^2)	0.28 ± 0.35	0.37 ± 0.38	0.31
% Fibrotic area	58.03 ± 13.43	58.25 ± 11.52	0.94
% Fibrofatty area	22.29 ± 16.41	17.21 ± 11.99	0.19
% Necrotic core area	15.34 ± 10.40	19.50 ± 9.48	0.07
% Dense calcium area	3.85 ± 5.23	5.05 ± 5.45	0.35
Remodeling Index	1.02 ± 0.22	0.94 ± 0.20	0.045
Distal reference segment			
EEM area (mm^2)	15.32 ± 6.05	13.24 ± 5.61	0.12
Lumen area (mm^2)	8.48 ± 3.72	7.33 ± 3.10	0.13
Plaque area (mm^2)	6.83 ± 2.97	6.29 ± 3.84	0.54

Values are presented as mean ± SD or percentages

MLA Minimum lumen area, *EEM* external elastic membrane, *VH-TCFA* Virtual histology thin-capped fibroatheroma

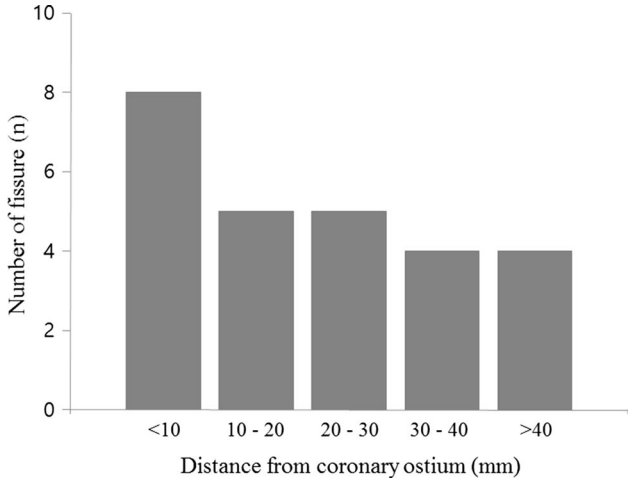

Fig. 4 Frequency distribution of the plaque fissure at the culprit lesion according to the distance from the coronary ostium

linear crack in the luminal surface of plaque where there is small necrotic core with limited extension into the necrotic core with residual little thrombus. The superficial tear lifts a layer of the intima from the underlying fibrous tissue and the hemorrhage extends into the necrotic core with difficult to appreciate thrombus in the lumen [6]. However, the terms "fissure and rupture" are interchangeable and stressed that a variable mix of hemorrhage into the plaque and luminal thrombosis originating from the fissure/rupture site characterizes culprit lesions in ACS [4]. Although the plaque fissure is a cause of plaque disruption as like plaque rupture and erosion, however, the term fissure is less well-defined. Of the pathophysiologic mechanism, the positive remodeling is typically considered indicative of an unstable lesion and negative remodeling indicative of stable coronary artery disease [22]. However, negative remodeling is a feature of plaque erosions and is not always benign, consistent with the data from PROSPECT [23].

In this study, we assessed a plaque fissure which shows a unique feature compared to ruptured plaque. The OCT finding of a plaque fissure is a creation of linear tear, however the ruptured cavity is represented in the plaque rupture. Compared to the rupture plaque, plaque fissure showed smaller necrotic core without ruptured cavity. Two third of the plaque fissure were associated with the lipidic plaque. Small lipidic plaque with limited extension into the lipid core provoke a fissuring of the plaque depends on the magnitude of wall tension which might be occurred in the situation of ACS. And the frequency of the positive remodeling was less in the plaque fissure compared to the plaque rupture.

This study has some limitations. First, this study was a small observational study. Second, the terminology of plaque fissure is rarely used due to its ambiguous definition, however this is the first study to demonstrate the plaque fissure using OCT. Third, the OCT findings of the plaque fissure were not validated by histopathology. Fourth, small coronary fissure can be identified only in diastole which can be disappeared in systole. The ECG gating may be helpful to identify the cardiac cycle, but it is not available in current OCT system. And we could not discriminate a small, tiny fissure due to the limited resolution of current OCT system. Fifth, we did not assess the entire coronary tree using OCT. Sixth, the accuracy of OCT and IVUS analysis is reduced in the presence of intracoronary thrombus. Seventh, the frequency of the plaque fissure might be reduced because we excluded the confused case such as microvessel (Fig. 3c). Finally, although we use the softest guidewire to reduce the vessel injury during PCI, however, it could not exclude the possibility of 'iatrogenic fissure' due to guidewire manipulation.

Conclusion

Although the plaque fissure and rupture can be interchangeable, however it might be another manifestation of the plaque disruption with the limited extension to the lipid core and less positive remodeling. Further study is necessary to assess the plaque fissure.

Acknowledgements The author thanks to YM Jo and DW Kang, researchers of Heart Research Institute, for their efforts to collect and review the cases, and KS Park, MPH, for her statistical assistance.

Compliance with ethical standards

Conflict of interest The authors declare that they have no conflict of interest.

References

1. Fuster V, Badimon L, Badimon JJ, Chesebro JH (1992) The pathogenesis of coronary artery disease and the acute coronary syndromes. N Eng J Med 326:310–318
2. Davies MJ (2000) The pathophysiology of acute coronary syndromes. Heart 83:361–366
3. Kolodgie FD, Virmani R, Burke AP, Farb A, Weber DK, Kutys R, Finn AV, Gold HK (2004) Pathologic assessment of the vulnerable human coronary plaque. Heart 90:1385–1391
4. Davies MJ, Thomas AC (1985) Plaque fissuring-the cause of acute myocardial infarction, sudden ischaemic death, and crescendo angina. Br Heart J 53:363–573
5. Balakrishnan KR, Kuruvilla S, Srinivasan A, Sehgal PK (2007) Electron microscopic insights into the vascular biology of atherosclerosis; study of coronary endarterectomy specimens. Circulation 115:e388–e390
6. Falk E, Nakano M, Bentzon JF, Finn AV, Virmani R (2013) Update on acute coronary syndromes: the pathologists' view. Eur Heart J 34:719–728
7. Kume T, Akasaka T, Yoshida K (2007) Optical coherence tomography after cutting balloon angioplasty. Heart 93:546

8. Kubo T, Imanishi T, Takarada S, Kuroi A, Ueno S, Yamano T, Tanimoto T, Matsuo Y, Masho T, Kitabata H, Tsuda K, Tomobuchi Y, Akasaka T (2007) Assessment of culprit lesion morphology in acute myocardial infarction: ability of optical coherence tomography compared with intravascular ultrasound and coronary angioscopy. J Am Coll Cardiol 50:933–939
9. Jang IK, Tearney GJ, MacNeill B, Takano M, Moselewski F, Iftima N, Shishkov M, Houser S, Aretz HT, Halpern EF, Bouma BE (2005) In vivo characterization of coronary atherosclerotic plaque by use of optical coherence tomography. Circulation 111:1551–1555
10. Pinto TL, Waksman R (2006) Clinical application of optical coherence tomography. J Interv Cardiol 19:566–573
11. Jia H, Abtahian F, Aguirre AD, Lee S, Chia S, Lowe H, Kato K, Yonetsu T, Vergallo R, Hu S, Tian J, Lee H, Park SJ, Jang YS, Raffel OC, Mizuno K, Uemura S, Itoh T, Kakuta T, Choi SY, Dauerman HL, Prasad A, Toma C, McNulty I, Zhang S, Yu B, Fuster V, Narula J, Virmani R, Jang IK (2013) In vivo diagnosis of plaque erosion and calcified nodule in patients with acute coronary syndrome by intravascular optical coherence tomography. J Am Coll Cardiol 62:1748–1758
12. Kwon JE, Lee WS, Mintz GS, Hong YJ, Lee SY, Kim KS, Hahn JY, Kumar KS, Won H, Hyeon SH, Shin SY, Lee KJ, Kim TH, Kim CJ, Kim SW (2016) Multimodality intravascular imaging assessment of plaque erosion versus plaque rupture in patients with acute coronary syndrome. Korean Circ J 46:499–506
13. Tearney GJ, Regar E, Akasaka T, Adriaenssens T, Barlis P, Bezerra HG, Bouma B, Bruining N, Cho JM, Chowdhary S, Costa MA, de Silva R, Dijkstra J, Di Mario C, Dudek D, Falk E, Feldman MD, Fitzgerald P, Garcia-Garcia HM, Gonzalo N, Granada JF, Guagliumi G, Holm NR, Honda Y, Ikeno F, Kawasaki M, Kochman J, Koltowski L, Kubo T, Kume T, Kyono H, Lam CC, Lamouche G, Lee DP, Leon MB, Maehara A, Manfrini O, Mintz GS, Mizuno K, Morel MA, Nadkarni S, Okura H, Otake H, Pietrasik A, Prati F, Räber L, Radu MD, Rieber J, Riga M, Rollins A, Rosenberg M, Sirbu V, Serruys PW, Shimada K, Shinke T, Shite J, Siegel E, Sonoda S, Suter M, Takarada S, Tanaka A, Terashima M, Thim T, Uemura S, Ughi GJ, van Beusekom HM, van der Steen AF, van Es GA, van Soest G, Virmani R, Waxman S, Weissman NJ, Weisz G (2012) International Working Group for Intravascular Optical Coherence Tomography (IWG-IVOCT) Consensus standards for acquisition, measurement, and reporting of intravascular optical coherence tomography studies: a report from the international working group for intravascular optical coherence tomography standardization and validation. J Am Coll Cardiol 59:1058–1072
14. Mintz GS, Nissen SE, Anderson WD, Bailey SR, Erbel R, Fitzgerald PJ, Pinto FJ, Rosenfield K, Siegel RJ, Tuzcu EM, Yock PG (2001) American College of Cardiology Clinical Expert consensus document on standards for acquisition, measurement and reporting of intravascular ultrasound studies (IVUS). A report of the American College of Cardiology Task Force on clinical expert consensus documents. J Am Coll Cardiol 37:1478–1492
15. Garcia-Garcia HM, Mintz GS, Lerman A, Vince G, Margolis MP, Es GV, Morkel MM, Nair A, Virmani R, Burke AP, Stone GW, Serruys PW (2009) Tissue characterisation using intravascular radiofrequency data analysis: recommendations for acquisition, analysis, interpretation and reporting. EuroIntervention 5:177–189
16. Richardson PD, Davies MJ, Born GV (1989) Influence of plaque configuration and stress distribution on fissuring of coronary atherosclerotic plaques. Lancet 2:941–944
17. Burke AP, Kolodgie FD, Farb A, Weber DK, Malcom GT, Smialek J, Virmani R (2001) Healed plaque ruptures and sudden coronary death: evidence that subclinical rupture has a role in plaque progression. Circulation 103:934–940
18. Wang JC, Normand SL, Mauri L, Kuntz RE (2004) Coronary artery spatial distribution of acute myocardial infarction occlusions. Circulation 110:278–284
19. Hong MK, Mintz GS, Lee CW, Lee BK, Yang TH, Kim YH, Song JM, Han KH, Kang DH, Cheong SS, Song JK, Kim JJ, Park SW, Park SJ (2005) The site of plaque rupture in native coronary arteries: a three-vessel intravascular ultrasound analysis. J Am Coll Cardiol 46:261–265
20. Fujii K, Masutani M, Okumura T, Kawasaki D, Akagami T, Ezumi A, Sakoda T, Masuyama T, Ohyanagi M (2008) Frequency and predictor of coronary thin-cap fibroatheroma in patients with acute myocardial infarction and stable angina pectoris a 3-vessel optical coherence tomography study. J Am Coll Cardiol 52:787–788
21. Toutouzas K, Karanasos A, Riga M, Tsiamis E, Synetos A, Michelongona A, Papanikolaou A, Triantafyllou G, Tsioufis C, Stefanadis C (2012) Optical coherence tomography assessment of the spatial distribution of culprit ruptured plaques and thin-cap fibroatheromas in acute coronary syndrome. EuroIntervention 8:477–485
22. Schoenhagen P, Ziada KM, Kapadia SR, Crowe TD, Nissen SE, Tuzcu EM (2000) Extent and direction of arterial remodeling in stable versus unstable coronary syndromes: an intravascular ultrasound study. Circulation 101:598–603
23. Inaba S, Mintz GS, Farhat NZ, Fajadet J, Dudek D, Marzocchi A, Templin B, Weisz G, Xu K, de Bruyne B, Serruys PW, Stone GW, Maehara A (2014) Impact of positive and negative lesion site remodeling on clinical outcomes: insights from PROSPECT. JACC Cardiovasc Imaging 7:70–78